Available online at http://scik.org
Commun. Math. Biol. Neurosci. 2019, 2019:17
https://doi.org/10.28919/cmbn/4058
ISSN: 2052-2541

AN ECOLOGICAL MODEL FOR SUSTAINABLE WILDLIFE MANAGEMENT OF THE SUNDARBANS' ECO-SYSTEM BASED ON OPTIMAL CONTROL THEORY

MD. NAZMUL HASAN[1,*], MD. HAIDER ALI BISWAS[2], MD. SHARIF UDDIN[1]

[1]Department of Mathematics, Jahangirnagar University, Savar, Dhaka, Bangladesh

[2] Mathematics Discipline, Khulna University, Khulna, Bangladesh

Abstract. The threats to wildlife in Sundarban, the largest mangrove forest in the world are poaching, recurrent coastal flooding, cyclone and toxicity. Optimal control theory is applied to investigate optimal strategies for controlling these threats in the system where anti-poaching patrols are used for poaching, strong Bomas are constructed to stopping retaliatory killing, green fence is built for controlling coastal flood and cyclone and re-rout is applied for toxicity control. The combination of the three controls is used to control its possible impact on the threats that the predator and the prey facing in Sundarbans. The system is also examined so that the best result is achieved. In this study, we have also analyzed the optimal control theory where the existing condition is discussed. However, different control strategies are considered and the achieved results are discussed together with the effect of variation of prey refuge.

Keywords: ecological model; intra-specific competition; local and global stability; Lyapunov function; control theory.

2010 AMS Subject Classification: 92D30, 92D40, 37B25, 34D23, 49K15.

[*]Corresponding author
E-mail address: nazmulmaths@gmail.com
Received March 13, 2019

1. Introduction

The Sundarban is the single largest mangrove forest in the world comprising a total area of 9827 sq. kms. lying in both Bangladesh and India. This reserve includes the Royal Bengal Tigers, swamp deer, snake, different type of alligator, monkeys, large number of birds fishing cats, water buffaloes etc. It is the only marshy mangrove land for included tigers in the world heritage sites. This area shows high biodiversity with unique flora and fauna. Some of the biological species have been driven to extinction tigers and many others are at the verge of extinction due to several external forces such as over exploitation predation, environmental pollution and mismanagement of habitat. These problems affecting wild animals and their habitats should be evaluated to ensure sustainable conservation of wildlife population.

Environmental pollution, poaching, catastrophes as mismanagement of the habitat may cause reduction of species population and lead to extinction due to perturbation of the system. Hazards such as coastal flooding and cyclone also cause the decline of species in an ecosystem. A number of species have become extinct during the last 100 years from the Sundarbans. It provides In-situ conservation of biodiversity of natural and semi-natural ecosystems and landscapes and contributes to sustainable economic development of the human population living within and around the biosphere reserve.

Bolger et al [19] mentioned poaching of wildlife as a main threat for the ecosystem. Poaching has become a threat to many migratory population, particularly as human populations around protected areas increases. It has been reported that the local consumption of bush meat from the Sundarbans and surrounding areas is responsible for the death of wild beasts per year and any further increase in the amount of poaching could lead to decline in the wild populations in the Sundarbans ecosystem. The predators (tiger) and the preys (deer) carry a dynamic relationship among themselves. For its universal existence and importance, this relationship is one of the dominant themes in theoretical ecology. In the context of Sundarbans, this relationship exists between tiger and deer. Mathematical modeling is considered a very useful tool to understand and analyze the dynamic behavior of predator-prey systems. Predator functional response on prey population is the major element in predator-prey interaction. It describes the number of prey consumed per predator per unit time for given quantities of prey and predator. The most important and useful functional responses are Holling type I functional response, Holling type II functional response and Ratio dependent functional response. The two species population models with such functional responses are widely researched in ecological environment. We consider two different populations species: x_1 as the prey population (deer) and x_2 as the predator (tiger) population. We also assume that both population species are threatened by poaching coastal flood and disease which are considered to affect their survival. Here we assume that the prey population are to grow logistically to the carrying capacity. We also assume that there is a refuge habitat where prey population are protected from predation and non-refuge habitat in which prey population are exposed to predation. Thus, for the ratio dependent functional response we make the following assumptions:

$$\frac{dx_1}{dt} = r_1x_1(1-\frac{x_1}{k}) - \frac{\mu(1-m)x_1x_2}{x_2+a(1-m)x_1} - p_1x_1 - q_1x_1 - \tau_1x_1, \tag{1a}$$

$$\frac{dx_2}{dt} = -r_2x_2 + \frac{e\mu(1-m)x_1x_2}{x_2+a(1-m)x_1} - p_2x_2 - q_2x_2 - \tau_2x_2^2, \tag{1b}$$

$$x_1(0) \geq 0, \quad x_2(0) \geq 0$$

where r_1 be the prey intrinsic growth rate, r_2 be the death rate of predator absence of prey, k be the carrying capacity of prey species, μ be the predation rate, e be the conversion factor $(0 < e < 1)$, m be the prey refuge parameter, that it protects mx_1 of the prey and leaves $(1-m)x_1$ of the prey available to the predator $(0 \leq m < 1)$, p_1 and p_2 be the poaching rates for prey and predator populations respectively, tau_1 and tau_2 be the rate of toxicity for both species respectively, q_1 and q_2 be the death rates due to coastal flood and other natural calamities for both species respectively.

Let $D_1 = p_1 + q_1$ and $D_2 = p_2 + q_2$ then the model system (1a)-(1b) becomes,

$$f_1(x_1,x_2) = \frac{dx_1}{dt} = r_1x_1(1-\frac{x_1}{k}) - \frac{\mu(1-m)x_1x_2}{x_2+a(1-m)x_1} - D_1x_1 - \tau_1x_1, \tag{2a}$$

$$f_2(x_1,x_2) = \frac{dx_2}{dt} = -r_2x_2 + \frac{e\mu(1-m)x_1x_2}{x_2+a(1-m)x_1} - D_2x_2 - \tau_2x_2^2, \tag{2b}$$

$$x_1(0) \geq 0, \quad x_2(0) \geq 0.$$

2. PRELIMINARIES

2.1. Boundedness.

Theorem 2.1. *All the solutions $(x_1(t), x_2(t))$ of the system (2a)-(2b) in R^2_+ are bounded.*

Proof. To prove the theorem, we define a function $z(t) = x_1(t) + \frac{1}{e}x_2(t)$.

Therefore, time derivative yields

$$\begin{aligned}\frac{dz}{dt} &= \frac{dx_1}{dt} + \frac{1}{e}\frac{dx_2}{dt}\\ &= r_1x_1(1-\frac{x_1}{k}) - D_1x_1 - \tau_1x_1 - \frac{1}{e}[(r_2+D_2)x_2 + \tau_2x_2^2]\\ &= (r_1 - D_1 - \tau_1)x_1 - \frac{r_1}{k}x_1^2 - \tau_1x_1^2 - \frac{1}{e}[(r_2+D_2x_2) + \tau_2x_2^2]\end{aligned}$$

$$\frac{dz}{dt} = x_1[(r_1 - D_1 - \tau_1) - \frac{r_1}{k}x_1] - \frac{1}{e}x_2[(r_2+D_2) + \tau_2x_2]. \tag{3}$$

Now $\frac{dz}{dt} + \eta z = x_1[(r_1 - D_1 - \tau_1 + \eta) - \frac{r_1}{k}x_1] + \frac{1}{e}x_2[(\eta - r_2 - D_2) + \tau_2x_2]$

$\leq \frac{k}{4r_1}(r_1 - D_1 - \tau_1 + \eta)^2 + \frac{1}{4e\tau_2}(\eta - r_2 - D_2)^2$ [using completing square technique]

implies $\frac{dz}{dt} + \eta z < M$ where $M = \frac{k}{4r_1}(r_1 - D_1) + \eta)^2 + \frac{1}{4e\tau_2}(\eta - r_2 - D_2)^2$.

Solving the resulting differential inequality with integrating factor, $I = e^{\eta t}$ we get $z(t) < \frac{M}{\eta} + ce^{-\eta t}$. At $t = 0, z(x_1(0), x_2(0)) = z$ and then from (3) we obtain, $z(x(0), y(0)) = \frac{M}{\eta} + c$ which implies that $z(t) \leq \frac{M}{\eta} + z(x(0), x_2(0)) - \frac{M}{\eta})e^{-\eta t}$

$= \frac{M}{\eta}(1 - e^{-\eta t} + z(x_1(0), x_2(0)))e^{-\eta t}$.

So, $0 \leq z(x_1(0), x_2(0)) \leq \frac{M}{\eta}(1 - e^{-\eta t}) + z(x_1(0), x_2(0))e^{-\eta t}$.

At $t \to \infty$, then $0 \leq z(x_1(t), x_2(t)) \leq \frac{M}{\eta}$.

Thus z is bounded and from positive of x_1 and x_2 where $0 \leq x_1 \leq M, 0 \leq x_2 \leq M$ for all $t > 0$. □

2.2. Dissipativeness.

Theorem 2.2.1. *If $w \geq \frac{a}{e}(r_2 + D_2)$ then the system (2a)-(2b) is dissipative.*

Proof. By usual straight forward arguments, we can show that the solution of the system (2a)-(2b) always exists and keeps on positive, Since all the interacting species and parameters associated with model system (2a)-(2b) are positive and $m \in [0, 1)$ now, from the first equation of

the model system (2a)-(2b) we have, $\frac{dx_1}{dt} < r_1 x_1(1-\frac{x_1}{k})$ consequently,
we observe that $x_1(t) \leq \frac{x_1(0)}{x_1(0)+(1-x_1(0))e^{-t}}$.
Thus, any any solution of the model system (2a)-(2b) must satisfy

$$\lim_{t\to\infty} sup x_1(t) < 1. \tag{4}$$

Again from the second equation of the model system (2a)-(2b), we examine that,

$$\begin{aligned}
\frac{dx_2}{dt} &= \frac{e\mu(1-m)x_1x_2}{x_2+a(1-m)x_1} - (r_2+D_2+\tau_2 x_2)\\
&= \frac{\frac{e\mu}{a}x_2}{\frac{x_2}{a(1-m)}+1} - (r_2+D_2+\tau_2 x_2)\\
&\leq \frac{e\mu}{a}x_2 - (r_2+D_2+\tau_2 x_2).
\end{aligned}$$

$$\therefore \frac{dx_2}{dt} \leq (\frac{e\mu}{a} - r_2 - D_2 - \tau_2 x_2). \tag{5}$$

Therefore we have

$$\lim_{t\to\infty} sup x_2(t) \leq \bar{x_2}, \tag{6}$$

where $\bar{x_2}$ denotes a unique solution of $x_2(t)$ which is positive if $\mu > \frac{a}{e}(r_2+D_2)$. □

2.3. Permanence.

Theorem 2.3.1. *If $\mu \geq \frac{a}{e}(r_2+D_2)$ then the system (2a)-(2b) is permanent.*

Proof. From the first equation of the model system (2a)-(2), we get,

$$\begin{aligned}
\frac{dx_1}{dt} &= r_1x_1(1-\frac{x_1}{k}) - \frac{\mu(1-m)x_1x_2}{x_2+a(1-m)x_1} - D_1x_1 - \tau_1 x_1\\
&= r_1x_1(1-\frac{x_1}{k}) - \frac{\mu(1-m)x_1}{1+a(1-m)\frac{x_1}{x_2}} - D_1x_1 - \tau_1 x_1\\
&\geq r_1x_1(1-\frac{x_1}{k}) - \mu(1-m)x_1 - D_1x_1 - \tau_1 x_1\\
&\geq \frac{r_1}{k}x_1[\frac{k}{r_1}(r_1 - D_1 - \tau_1 - \mu(1-m) - \frac{(r_1+k\tau_1)}{k}x_1]
\end{aligned}$$

$$\therefore \frac{dx_1}{dt} \geq \frac{k}{4r_1}[r_1 - D_1 - \tau_1 - \mu(1-m)]^2. \tag{7}$$

Hence, for large t we choose, $x_1(t) = \frac{\bar{x}_1}{3}$.

$\therefore \frac{dx_2}{dt} = \frac{e\mu(1-m)x_1x_2}{x_2+a(1-m)x_1} - (r_2+D_2+\tau_2x_2)x_2$.

If x_2 is the root of the equation $x_2[\frac{e\mu(1-m\bar{x})}{a(3x_2+(1-m)\bar{x}} - (r_2+D_2+\tau_2x_2)] = 0$

$\therefore x_2 = \frac{e\mu - a(r_2+D_2)(1-m)\bar{x}_1}{r_2+D_2}$

Therefore, we obtain

$$\lim_{t\to\infty} inf x_2(t) \geq \bar{x}_2 \tag{8}$$

if $\mu \geq \frac{a}{e}(r_2+D_2)$ □

2.4. Equilibrium Analysis. In this section we establish the conditions for the existence of the four equilibrium points of the model system namely $E_0(x_{10}, x_{20}), E_1(x_{11}, x_{21}), E_2(x_{12}, x_{22})$ and $E_3(x_{13}, x_{23})$.

(a) Predator- prey extinction equilibrium point: When the predator and prey do not exists i.e., $x_1 = x_2 = 0$ thus the equilibrium point is obtained $E_0(x_{10}, x_{20}) = E_0(0,0)$.

(b) Predator extinction equilibrium point: When there are no predator i.e., $x_1 \neq 0$ and $x_2 = 0$ then from the system (2a)-(2b) we get,

$$\begin{aligned}
&\frac{dx_1}{dt} = 0\\
&\Rightarrow r_1x_1(1-\frac{x_1}{k}) - D_1x_1 - \tau_1x_1 = 0\\
&\Rightarrow \frac{r_1x_1}{k} = r_1 - D_1 - \tau_1\\
&\Rightarrow x_1 = \frac{k}{r_1}(r_1 - D_1 - \tau_1).
\end{aligned} \tag{9}$$

Thus the equilibrium point is obtained $E_1(x_{11}, x_{21}) = E_1\big(\frac{k}{r_1}(r_1 - D_1 - \tau_1), 0\big)$.

Therefore, from the fact $x_1 > 0$ the equilibrium E_1 exists if $r_1 > D_1$ i.e., $r_1 > p_1 + q_1 + d_1$.

Thus in the absence of predator species x_2, the total prey death rate due to threats must be less than its intrinsic growth rate for the point $E_1(x_1, 0)$ to exists.

(c) Prey extinction equilibrium point: Where there are no prey i.e., $x_1 = 0$ and $x_2 \neq 0$ then from the system (2a)-(2b) we get,

$$\frac{dx_2}{dt} = 0$$
$$\Rightarrow x_2(r_2 + D_2 + \tau_2 x_2) = 0$$
$$\Rightarrow x_2 = -\frac{r_2 + D_2}{\tau_2} \tag{10}$$

Thus the equilibrium point is obtained $E_2(x_{12}, x_{22}) = E_2(0, -\frac{r_2+D_2}{\tau_2})$

This result shows that the model assumption that the predator's only the source of prey, then the predator goes to extinction.

(d) Co-existence equilibrium point: When Predator and prey i.e., both species co-exists i.e., $x_1 \neq 0, x_2 \neq 0$ then from the system (2a)-(2b) we have, $\frac{dx_1}{dt} = 0$ and $\frac{dx_2}{dt} = 0$.

3. Dynamic Behavior of the System

3.1. Local Stability Analysis. In this section we analysis the stability properties of the equilibrium points E_0, E_1, E_2 and E_3. The local stability is established through Jacobian matrix of the system and finding the eigenvalues to evaluate at each equilibrium point. For linearized system the Jacobian matrix is given by, $\begin{vmatrix} \frac{\partial f_1}{\partial x_1} & \frac{\partial f_1}{\partial x_2} \\ \frac{\partial f_2}{\partial x_1} & \frac{\partial f_2}{\partial x_2} \end{vmatrix}$.

For the model system (2a)-(2b) its corresponding Jacobian matrix is $J(E_i) = \begin{vmatrix} J_{11} & J_{12} \\ J_{21} & J_{22} \end{vmatrix}$,

where $J_{11} = -D_1 - \frac{r_1 x_1}{k} + r_1(1 - \frac{x_1}{k}) + \frac{a(1-m)^2 \mu x_1 x_2}{(a(1-m)x_1+x_2)^2} - \frac{(1-m)\mu x_2}{a(1-m)x_1+x_2}$,

$J_{12} = \frac{(1-m)\mu x_1 x_2}{(a(1-m)x_1+x_2)^2} - \frac{(1-m)\mu x_1}{a(1-m)x_1+x_2}$,

$J_{21} = \frac{(1-m)^2 \mu x_1 x_2}{(a(1-m)x_1+x_2)^2} + \frac{e(1-m)\mu x_2}{a(1-m)x_1+x_2}$,

$J_{22} = -D_2 - r_2 - 2\tau_2 x_2 - \frac{e(1-m)\mu x_1 x_2}{(a(1-m)x_1+x_2)^2} + \frac{e(1-m)\mu x_1}{a(1-m)x_1+x_2}$.

3.2. Behavior of the system around the origin $E_0(0,0)$. The Jacobian matrix J_0 at $E_0(0,0)$ is

$$J(E_0) = \begin{vmatrix} r_1 - D_1 & 0 \\ 0 & -(r_2 + D_2) \end{vmatrix}.$$

The eigenvalue of the Jacobian matrix at $E_0(0,0)$ are $r_1 - D_1$ and $-(r_2 + D_2)$. Hence the equilibrium point $E_0(0,0)$ unstable saddle point.

3.3. Behavior of the system around the origin $E_1(x,0)$. The Jacobian matrix J_1 at $E_0(x_1,0)$ is

$$J(E_1)=\begin{vmatrix} -D_1-\frac{r_1x_1}{k}+r_1(1-\frac{x_1}{k}) & -\frac{\mu}{a} \\ 0 & -(r_2+D_2-\frac{e\mu}{a}) \end{vmatrix}.$$

The eigenvalue of the Jacobian matrix at $E_1(x_1,0)$ are $-D_1-\frac{r_1x_1}{k}+r_1(1-\frac{x_1}{k})$ and $-(r_2+D_2-\frac{e\mu}{a})$. Hence the equilibrium point $E_1(x_{10},0)$ unstable saddle point.

3.4. Behavior of the system around the origin $E_2(0,x_{22})$. The Jacobian matrix J_2 at $E_0(0,x_{22})$ is

$$J(E_2)=\begin{vmatrix} -D_1-r_1-\tau_1-(1-m) & 0 \\ e\mu(1-m) & -(r_2+D_2+2\tau_2x_{22}) \end{vmatrix}.$$

Eigenvalues corresponding to the point $E_3(x_{13},x_{23})$ are the roots of the equation

$\lambda^2-\lambda(J_{11}+J_{22})+J_{11}J_{22}=0$

where, $J_{11}=-D_1-\frac{r_1x_{13}}{k}+r_1(1-\frac{x_{13}}{k})+\frac{a(1-m)^2\mu x_{13}x_{23}}{(a(1-m)x_{13}+x_{23})^2}-\frac{(1-m)\mu x_{23}}{a(1-m)x_{13}+x_{23}}$,

and $J_{22}=-D_2-r_2-2\tau_2x_{23}-\frac{e(1-m)\mu x_{13}x_{23}}{(a(1-m)x_{13}+x_{23})^2}+\frac{e(1-m)\mu x_{23}}{a(1-m)x_{13}+x_{23}}$.

3.5. Global Stability. To show the global stability of the system (2.2) we construct a Lyanpnov function as follows,

$L(x_1,x_2)=L_1(x_1-x_{23}-x_{13}log_e\frac{x_1}{x_{13}})+L_2(x_2-x_{23}-x_{23}log_e\frac{x_2}{x_{23}})$

where L_1 and L_2 be positive constants to be determined. We can easily verify that the function $L(x_1,x_2)=0$ at $E_3(x_{13},x_{23})$ and is positive for all other values of x_1 and x_2. Then the time derivative of $L(x_1,x_2)$ along the solution of the system is,

$$\begin{aligned}
\frac{dL}{dt}&=L_1(\frac{x_1-x_{13}}{x_1})\frac{dx_1}{dt}+L_2(\frac{x_2-x_{23}}{x_2})\frac{dx_2}{dt}\\
&=L_1[\frac{x_1-x_{13}}{x_1})x_1[r_1(1-\frac{x_1}{k})-\frac{\mu(1-m)x_2}{x_2+a(1-m)x_1}-D_1]\\
&+L_2(\frac{x_2-x_{23}}{x_2})x_2[r_2+\frac{e\mu(1-m)x_2}{y+a(1-m)x_2}-D_2-\tau_2x_2]\\
&=L_1(x_1-x_{13})[r_1(1-\frac{x_1}{k})-\frac{\mu(1-m)x_2}{x_2+a(1-m)x_1}-D_1-tau_1]\\
&+L_2(x_2-x_{23})[-r_2+\frac{e\mu(1-m)x_2}{x_2+a(1-m)x_1}-D_2-\tau_2x_2]
\end{aligned}$$

We have also the set of equilibrium equation corresponding the steady state point $E_3(x_{13}, x_{23})$.

$$
\begin{aligned}
&= L_1(x_1 - x_{13})\Big[r_1 - D_1 - \tau_1 - \frac{r_1 x_1}{k} - \frac{\mu(1-m)x_2}{x_2 + a(1-m)x_1}\Big] \\
&+ L_2(x_2 - x_{23})\Big[\frac{e\mu(1-m)x_2}{x_2 + a(1-m)x_1} - r_2 - D_2 - \tau_2 x_2\Big] \\
&= L_1(x_1 - x_{13})\Big[r_1 - D_1 - \tau_1 - \frac{r_1 x_1}{k} - \frac{\mu(1-m)x_2}{x_2 + a(1-m)x_1} - r_1 + -D_1 + \tau_1 - \frac{r_1 x_{13}}{k} + \frac{\mu(1-m)x_{13}}{x_{13} + a(1-m)x_{13}}\Big] \\
&+ L_2(x_2 - x_{23})\Big[\frac{e\mu(1-m)x_2}{x_2 + a(1-m)x_1} - r_2 - D_2 - \tau_2 x_2 - \frac{e\mu(1-m)x_{23}}{x_2 + a(1-m)x_{13}} + r_2 + D_2 + \tau_2 x_{23}\Big] \\
&= L_1(x_1 - x_{13})\Big[\frac{\mu(1-m)x_{23}}{x_{23} + a(1-m)x_{13}} - \frac{\mu(1-m)x_2}{x_2 + a(1-m)x_1} + \frac{r_1}{k}(x_{13} - x)\Big] \\
&+ L_2(x_2 - x_{23})\Big[\frac{e\mu(1-m)x_2}{x_2 + a(1-m)x_1} - \frac{e\mu(1-m)x_{23}}{x_{23} + a(1-m)x_{13}} + \tau_2(x_2 - x_{23})\Big] \\
&= L_1(x_1 - x_{13})\Big[\mu(1-m)\Big(\frac{x_{23}}{x_{23} + a(1-m)x_{13}} - \frac{x_2}{x_2 + a(1-m)x_1}\Big) + \frac{r_1}{k}(x_{13} - x_1)\Big] \\
&+ L_2(x_2 - x_{23})\Big[e\mu(1-m)\Big(\frac{x_2}{x_2 + a(1-m)x_1} - \frac{x_{23}}{x_{23} + a(1-m)x_{13}}\Big) + \tau_2(x_2 - x_{23})\Big] \\
&= L_1(x_1 - x_{13})\Big[\mu(1-m)\Big(\frac{x_{23}x_2 + a(1-m)x_1x_{23} - x_{23}x_2 - a(1-m)x_{13}x_2}{\big(x_{23} + a(1-m)x_{13}\big)\big(x_2 + a(1-m)x_1\big)}\Big) + \frac{r_1}{k}(x_{13} - x_1)\Big] \\
&+ L_2(x_2 - x_{23})\Big[e\mu(1-m)\Big(\frac{x_{23}x_2 + a(1-m)x_{13}x_2 - x_{23}x_2 - a(1-m)x_1x_{23}}{\big(x_{23} + a(1-m)x_{13}\big)\big(x_2 + a(1-m)x_1\big)}\Big) + \tau_2(x_2 - x_{23})\Big] \\
&= L_1(x_1 - x_{13})\Big[\frac{\mu a(1-m)^2(x_1x_{23} - x_{13}x_2)}{\big(x_{23} + a(1-m)x_{13}\big(x_2 + a(1-m)x_2\big)} + \frac{r_1}{k}(x_{13} - x)\Big] \\
&+ L_2(x_2 - x_{23})\Big[\frac{e\mu(1-m)^2(x_{13}x_2 - x_1x_{23})}{\big(x_{23} + a(1-m)x_{13}\big)\big(x_2 + a(1-m)x_1\big)} + \tau_2(x_2 - x_{23})\Big] \\
&= \frac{\mu a(1-m)^2(x_1x_{23} - x_{13}x_2)}{\big(x_{23} + a(1-m)x_{13}\big)\big(x_2 + a(1-m)x_1\big)}\Big[L_1(x_1 - x_{13}) - L_2(x_2 - x_{23})\Big] \\
&- \frac{r_1}{k}L_1(x_1 - x_{13})^2 + L_2\tau_2(x_2 - x_{23})^2 \\
&\therefore \frac{dL}{dt} \le \mu a(1-m)^2(x_1x_{23} - x_{13}x_2)\big[L_1(x_1 - x_{13}) - L_2(x_2 - x_{23})\big] \\
&- \frac{r_1}{k}L_1(x_1 - x_{13})^2 + L_2\tau_2(x_2 - x_{23})^2
\end{aligned}
$$

Let $L_1 = 1$ and $L_2 = \frac{x_1 - x_{13}}{x_2 - x_{23}}$ then we get,

$\frac{dL}{dt} \le \mu a(1-m)^2(x_1x_{23} - x_{13}x_2)\big[(x_1 - x_{13}) - (x_1 - x_{13})\big] - \frac{r_1}{k}(x_1 - x_{13})^2 + \tau_2(x_2 - x_{23})^2.\big(\frac{x_1 - x_{13}}{x_2 - x_{23}}\big)$

$\le \tau_2(x_2 - x_{23})(x_1 - x_{13}) - \frac{r_1}{k}(x_1 - x_{13})^2$

$\le (x_1 - x_{13})\big[h(x_2 - x_{23}) - \frac{r_1}{k}\big]$

$\therefore \frac{dL}{dt} < 0$ if $\tau_2(x_2 - x_{23}) - \frac{r_1}{k} > 0$.

Implies, $r_1 < \tau_1 k(x_2 - x_{23})$

and $\frac{dL}{dt} = 0$ iff $(x_1, x_2) \equiv (x_{13}, x_{23})$.

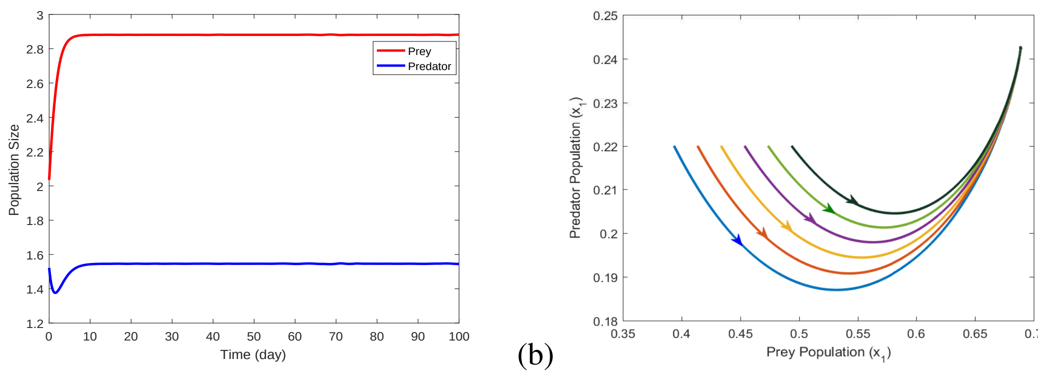

(a) (b)

FIGURE 1. Stability behaviour of the system (2a)-(2b) around the equilibrium position E_3 with the initial conditions $x_{10} = 2.50,\ x_{20} = 1.20$, (a) Time series, (b) Phase portrait.

3.6. Hopf-bifurcation Analysis.

At the equilibrium point $E_3(x_{13}, x_{23})$, the characteristic equation is given by,

$$\lambda^2 - (J_{11} + J_{22}) + (J_{11}J_{22} - J_{12}J_{21}) = 0$$

$$\Rightarrow \lambda^2 - (trJ_{E_3}) + (detJ_{E_3}) = 0 \tag{11}$$

where, $x_1 - x_{13} \approx e^{x_1 t}, x_2 - x_{23} \approx e^{x_2 t}$.

If $tr(J_{E_3}) = J_{11} + J_{22} = 0$ at $e = e_{[HB]}$, then both the positive eigenvalues are purely imaginary if $det(J_{E3}) = (J_{11}J_{22} - J_{12}J_{21})$ is positive.

Let the root of the corresponding characteristic equations are given by $\lambda = w_1(e) + iw_2(e)$ and $\lambda_2 = w_1(e) - iw_2(e)$.

Now substituting $\lambda = w_1(e) + iw_2(e)$ in the characteristic equation we get,

$$w_1^2 - w_2^2 + 2iw_1w_2 - tr(J_{E_3})(w_1 + iw_2) + det(J_{E_3}) = 0. \tag{12}$$

Equating the real and imaginary part, we get,

$$w_1^2 - w_2^2 - tr(J_{E_3})w_1 + det(J_{E_3}) = 0$$

$$2w_1w_2 - tr(J_{E_3}w_2) = 0. \tag{13}$$

Differentiating (15) with respect to e we get,

$$2\Big(\frac{dw_1}{de}w_2+\frac{dw_2}{de}w_1\Big)-\Big(\frac{dw_2}{de}tr(J_{E_3})+w_2\frac{d}{de}tr(J_{E_3})\Big)=0. \tag{14}$$

If $tr(J_{E_3})=0$ and if we consider $w_1=0$ we get,

$\Rightarrow 2\frac{dw_1}{de}w_2-w_2\frac{d}{de}tr(J_{E_3})=0$

$\Rightarrow \frac{dw_1}{de}=\frac{1}{2}\frac{d}{de}tr(J_{E_3})$

$=\frac{1}{2}\Big[\frac{(1-m)\mu x_{13}}{a(1-m)x_{13}+x_{23}}-\frac{(1-m)\mu x_{13}x_{23}}{\big(a(1-m)x_{13}+x_{23}\big)^2}\Big]$

$=\frac{1}{2}\Big(\frac{a(1-m)^2\mu x_{13}^2}{\big(a(1-m)x_1+x_2\big)^2}\Big)\neq 0.$

Hence, the system attains a Hopf bifurcation around the point $E_3(x_{13},x_{23})$ at $e=e_{[HB]}$, where $e_{[HB]}=\frac{\big(a(1-m)x_1+x_2\big)\big((D_1+D_2)-(r_1-r_2)+2\tau_2x_2+2x_1(\frac{r_1}{k})\big)}{a\mu(1-m)^2x_1^2}$

4. Ecological Model with Control

In order to show the controlling effect of threatened to the system, we consider anti-poaching patrol u_1, construction of strong green fence and Bomas u_2 and vaccination u_3 then reformulate the system (2a)-(2b) is,

$$\dot{x_1}=r_1x_1(1-\frac{x_1}{k})-\frac{w(1-m)x_1x_2}{x_2+a(1-m)x_1}-(1-u_1(t))p_1x_1-(1-u_2(t))q_1x_1 -(1-u_3(t))\tau_1x_1 \tag{15}$$

$$\dot{x_2}=-r_2x_2+\frac{ew(1-m)x_1x_2}{x_2+a(1-m)x_1}-(1-u_1(t))p_2x_2-(1-u_2(t))q_2x_2-(1-u_3)\tau_2x_2^2 \tag{16}$$

where $0\leq u_1\leq 1, 0\leq u_2\leq 1, 0\leq u_3\leq 1$.

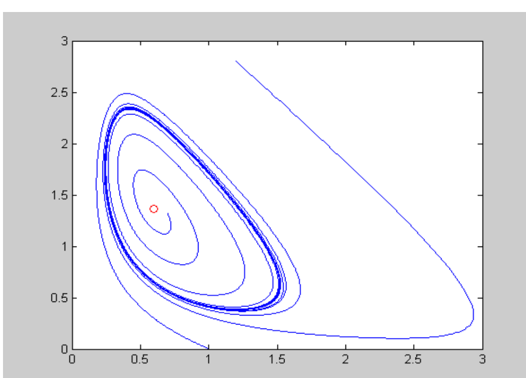

FIGURE 2. Hopf-bifurcation around the positive interior equilibrium point E_3.

4.1. Behavior of the control system. According to Pontryagin's maximum principle convert the system into a maximizing pointwise Hamiltonian H with respect to $u_1, u_2, u_3 \in U$ we get,
$H(t,x,u,\lambda) = \big(\gamma_1 \frac{u_1^2}{2} + \gamma_2 \frac{u_2^2}{2} + \gamma_3 \frac{u_3^2}{2}\big) + \lambda_1\{r_1 x_1(1-\frac{x_1}{k}) - \frac{w(1-m)x_1x_2}{x_2+(1-m)x_1} - \big(1-u_1(t)\big)p_1x_1 - \big(1-u_2(t)\big)q_1x - \big(1-u_3(t)\big)d_1x_1\} + \lambda_2\{-r_2x_2 + \frac{ew(1-m)x_1x_2}{x_1+(1-m)x_1} - \big(1-u_1(t)\big)p_2x_2 - \big(1-u_2(t)\big)q_2x_2 - \big(1-u_3(t)\big)d_2x_2 - hx_2^2\}$, where λ_1 and λ_2 be the adjoint variables.

Now applying Pontryagin's maximum principle [15] and the existence results for the optimal control [10] we obtained the following proposition,

Proposition: Maximizes $J(u_1,u_2,u_3)$ over U for the optimal control triple u_1^*, u_2^* and u_3^* then there exists adjoint variables λ_1 and λ_2 satisfying

$$\frac{d\lambda_1}{dt} = -\frac{\partial H}{\partial x_1} = -\Big[\lambda_1\Big\{r_1(1-\frac{2x_1}{k}) - \frac{\mu x_2^2(1-m)}{\big(x_2+a(1-m)x_1\big)^2}\Big\} - \Big\{(1-u_1)p_1 + (1-u_2)q_1 + (1-u_3)d_1\Big\} + \lambda_2\Big\{\frac{e\mu x_2^2(1-m)^2}{\big(x_2+(1-m)x_1\big)^2}\Big\}\Big]$$

$$\frac{d\lambda_2}{dt} = -\frac{\partial H}{\partial x_2} = -\Big[\lambda_1\Big\{r_1(\frac{\mu x_1^2(1-m)^2-1}{\big(x_2+a(1-m)x_1\big)^2}\Big\} + \lambda_2\Big\{-r_2\frac{e\mu x_1^2(1-m)^2}{\big(x_2+(1-m)x_1\big)^2}\Big\} - \Big\{(1-u_1)p_1 + (1-u_2)q_1 + (1-u_3)d_1 + 2hx_2\Big\}\Big]$$

and with transversality condition as $\lambda_1(T) = \delta_1$ and $\lambda_2(T) = \delta_2$ Using optimality condition, we have, $\frac{\partial H}{\partial u} = 0$ at u^*.
i.e, $\frac{\partial H}{\partial u_1} = 0$ at $u_1^*, \frac{\partial H}{\partial u_2} = 0$ at u_2^*, and $\frac{\partial H}{\partial u_3} = 0$ at u_3^*.
But $\frac{\partial H}{\partial u_1} = -\gamma_1 u_1 + \lambda_1 x_1 p_1 + \lambda_2 p_2 x_2 = 0$ at u_1^*.
Hence $u_1^* = \frac{L_1 p_1 x_1 + \lambda_2 P_2 y}{\gamma_1}$
$\frac{\partial H}{\partial u_2} = -\gamma_2 u_2 + \lambda_1 q_1 x_1 + \lambda_2 q_2 x_2 = 0$ at u_2^*.
Hence $u_2^* = \frac{\lambda_1 q_1 x + \lambda_2 q_2 y}{\gamma_2}$,
and $\frac{\partial H}{\partial u_3} = -\gamma_3 u_3 + \lambda_1 d_1 x_1 + \lambda_2 d_2 x_2 = 0$ at u_3^*.
Hence $u_3^* = \frac{\lambda_1 d_1 x + \lambda_2 d_2 y}{\gamma_3}$.
On the interior of the control set U the following characterization holds,
Note that the initial time condition and final time condition have in the state system (A) and co-state system (B) respectively.

5. Numerical simulation

Analytical studies could never be completed without numerical verification of the derived results. In this section, we have presented computer simulations of some solutions to the system (2a)-(2b). Along with the verification of our analytical findings, these numerical simulations are very important from practical point of view. We have used various forms of optimal strategies that can be applied to control the threatened predator-prey system. State system, co-state system and optimal characterization in the model system (2a)-(2b), (17) and (18) respectively are solved numerically in the following ways:

(a) Firstly divide the total time interval into n equal subintervals and set the state at different times as $\bar{x} = (x-1, x_2, \ldots.., x_{n+1})$ and the co-state variables as $\bar{L} = (L_1, L_2, \ldots.., L_{n+1})$.

(b) For starting iteration we assume control takes zero over the time interval i.e., $\bar{u} = (0, 0, ..., 0)$.

(c) Solve the state according to the ODE with the values of $\bar{u}$ forwardly by using the initial condition $x(0) = x_0$.

(d) Solve $\bar{L}$ in time from co-state differential equation in backward process by using the transversality condition $Ł_{n+1} = L(T)$, and the values of $\bar{u}$ is previously evaluated.

(e) Entering the new values of $\bar{x}$ and $\bar{L}$ and update the control through the rule

$u^* = min\big(u_{max}, max(u_{sig}, u_{min})\big)$

where

$$u^* = \begin{cases} u_{min} \text{ if } \frac{\partial H}{\partial u} < 0, \\ u_{sig} \text{ if } \frac{\partial H}{\partial u} = 0, \\ u_{max} \text{ if } \frac{\partial H}{\partial u} > 0. \end{cases}$$

(f) If the solution of the variables are convergent i.e., the values of the variables of the last iteration are negligibly close, then the solution is complete, otherwise return to step (c).

From different combinations of the controls, numerically we obtained seven strategies with $m = 0.021, m \in [0, 1)$.

5.1. Optimal control strategies.

Strategy (a) Application of anti-poaching patrols for controlling poaching. In this strategy, we use only anti-poaching patrols $u_1 \neq 0$ to optimize the objective function J, while construction of green fence and Bomas $u_2 = 0$ and use of vaccine $u_3 = 0$. In the FIGURE 3 we investigate the results that show significant difference between the predator-prey populations with the application of optimal control strategy and without the application. This shows that the predator-prey population size increases directly if poaching in the system is eliminated. Here we see that the optimal control anti-poaching patrol control u_1 increases gradually till time $t = 10$ years.

Strategy (b) Construction of strong Bomas and green fence. In this strategy we use only the

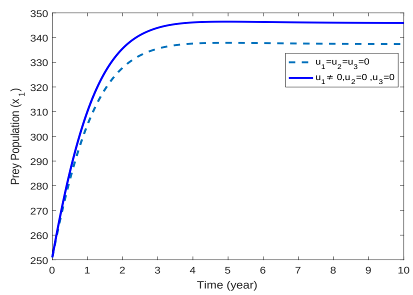

(a)

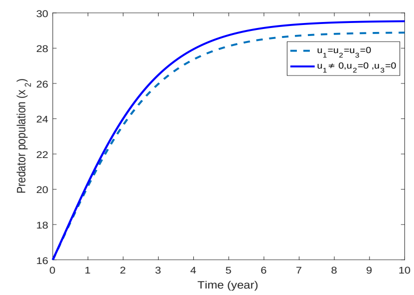

(b)

FIGURE 3. Simulations of a threatened predetor-prey model showing the effect of optimal application of anti-poaching patrols.

control of construction of strong Bomas and green fence $u_2 \neq 0$ to optimize the objective function J, while anti-poaching patrol $u_1 = 0$ and use of vaccines $u_3 = 0$. In the FIGURE 4 we investigate the results that show significant difference between the predator-prey populations with the application of optimal control strategy and without the application. This shows that the predator-prey population size increases directly if construction of strong bomas and green fence in the system.

Strategy (c) The use of vaccines for control of diseases. In this strategy we use only the control

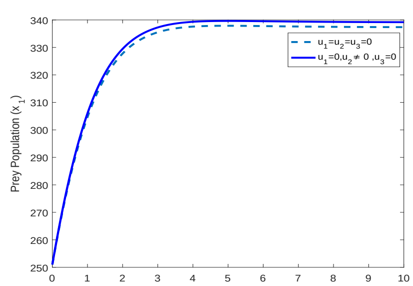

(a)

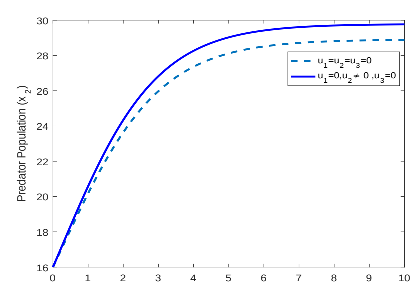

(b)

FIGURE 4. Simulations of a threatened predetor-prey model showing the effect of optimal application of strong Bomas and green fence.

of construction of strong Bomas and green fence $u_3 \neq 0$ to optimize the objective function J, while anti-poaching patrol $u_1 = 0$ and use of vaccines $u_2 = 0$. In the FIGURE 5 we investigate the results that show significant difference between the predator-prey populations with the application of optimal control strategy and without the application. This shows the predator- prey population size increases directly if use of vaccines in the system.

Strategy (d) Apply the combination of anti-poaching patrols and construction of Bomas and

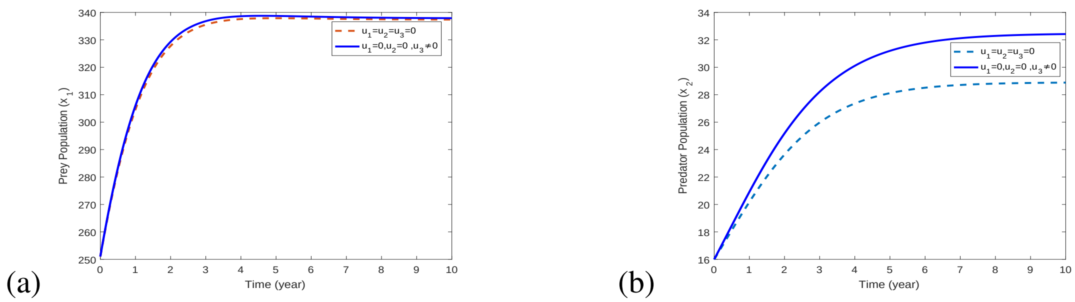

FIGURE 5. Simulations of a threatened predetor-prey model showing the effect of optimal application of vaccines.

green fence. In this strategy we use the control of construction of strong Bomas and green fence $u_2 \neq 0$ anti-poaching patrol $u_1 \neq 0$ to optimize the objective function J, while use of vaccines $u_3 = 0$. In the FIGURE 6 we investigate the results that show significant difference between the predator-prey populations with the application of optimal control strategy and without the application. This shows the predator-prey population size increases directly if construction of strong bomas and green fence and poaching in the system is eliminated.

Strategy (e) Apply the combination of anti-poaching patrols and construction of Bomas and

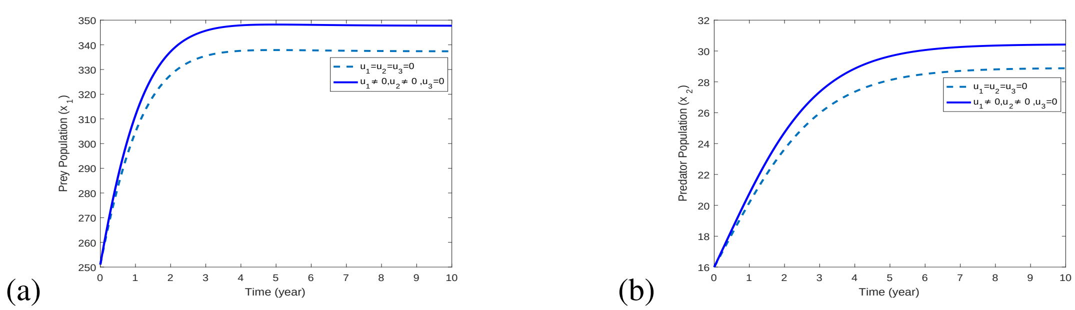

FIGURE 6. Simulations of a threatened predetor-prey model showing the effect of optimal application of anti-poaching patrols and construction of Bomas and green fence.

green fence. In this strategy we use the control of vaccines $u_3 \neq 0$ anti-poaching patrol $u_1 \neq 0$ to optimize the objective function J, while anti-poaching patrol $u_1 = 0$ and use of vaccines $u_3 = 0$. In the FIGURE 7 we investigate the results that show significant difference between the predator-prey populations with the application of optimal control strategy and without the application. This shows the predator-prey population size increases directly if use of vaccines and poaching in the system is eliminated.

Strategy (f) Apply the combination of anti-poaching patrols and use of vaccines. In this strat-

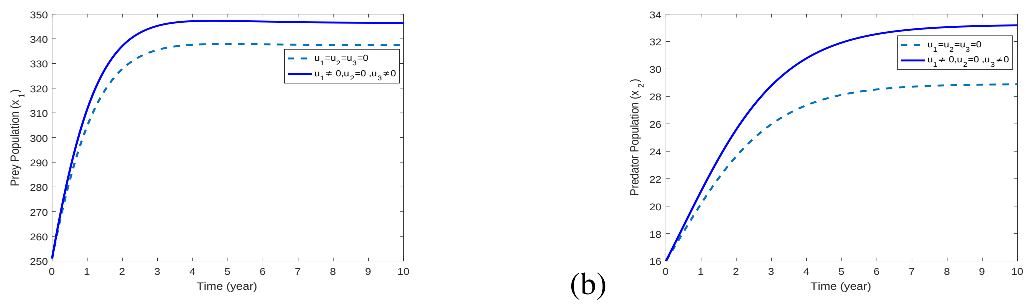

(a) (b)

FIGURE 7. Simulations of a threatened predetor-prey model showing the effect of optimal application of anti-poaching patrols and construction of Bomas and green fence.

egy we use the control of construction of strong bomas and green fence $u_2 \neq 0$ and the use of vaccines $u_3 \neq 0$ to optimize the objective function J, while anti-poaching patrol $u_1 = 0$ and use of vaccines $u_3 = 0$. In the FIGURE 8 we investigate the results that show significant difference between the predator-prey populations with the application of optimal control strategy and without the application. This shows the predator-prey population size increases directly if construction of strong bomas and green fence and the use of vaccines.

Strategy (g) Apply the combination of anti-poaching patrols, construction of strong Bomas and green fence and use of vaccines. In this strategy we use the control of anti-poaching patrols $u_1 \neq 0$ construction of strong Bomas and green fence $u_2 \neq 0$ and use of vaccines $u_3 \neq 0$ to optimize the objective function J. In the FIGURE 9 we investigate the results that show significant difference between the predator-prey populations with the application of optimal control strategy without the application. This shows that the predator- prey population size increases directly if combination of anti-poaching patrols, construction of strong Bomas and green fence

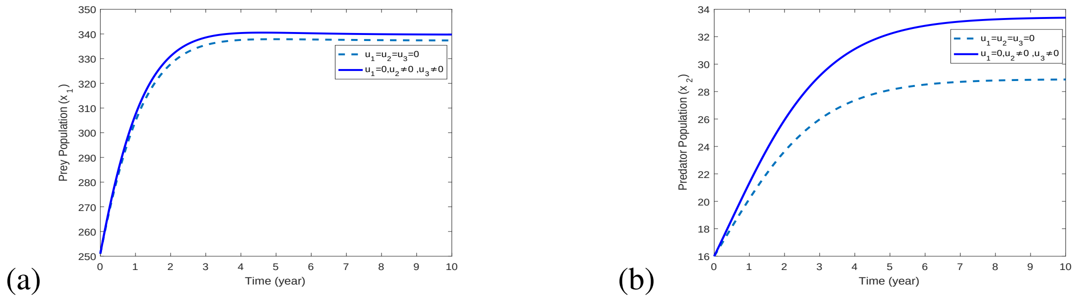

FIGURE 8. Simulations of a threatened predetor-prey model showing the effect of optimal application of anti-poaching patrols and use of vaccines.

and use of vaccines.

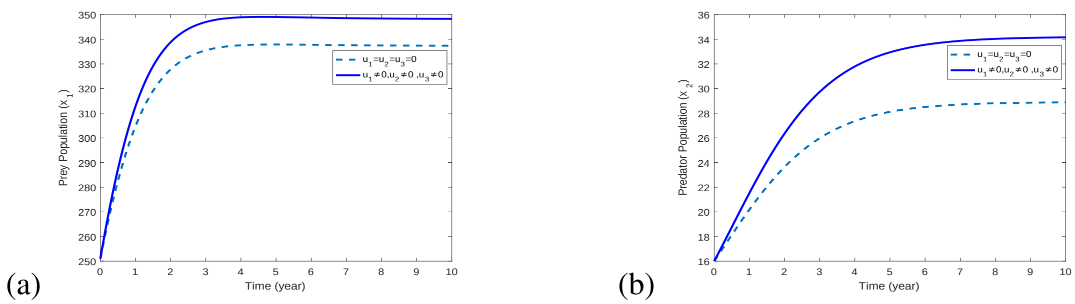

FIGURE 9. Simulations of a threatened predetor-prey model showing the effect of optimal application of anti-poaching patrols, contruction of strong Bomas and green fence and use of vaccines.

5.2. Effect of variation of refuge m.

In this section, we investigate the effect of variation of refuge m to optimal control strategies numerically.

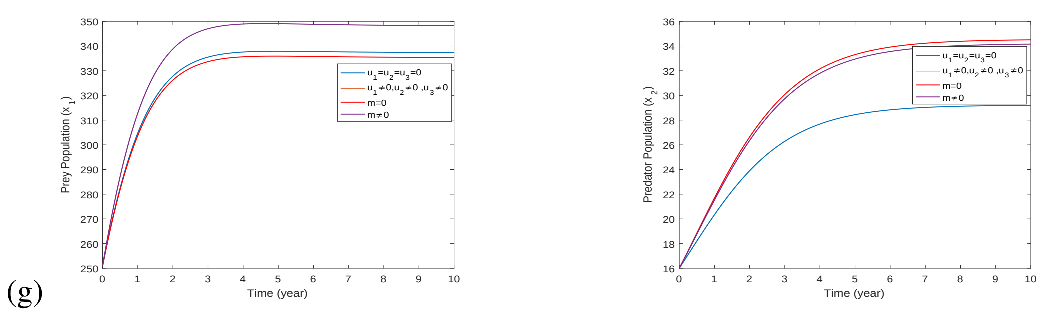

FIGURE 10. Effect of prey refuge m.

6. Conclusion

In this paper, we have presented a threatened fishery model using a deterministic system of differential equations. The threats are poaching and external toxicity. Ratio dependent response is used for the problems discussed in this study. The local and global stability conditions are obtained. Controls are introduced to the system which are anti-poaching patrols for controlling poaching, filtration and re-route of toxic fumes in the water vehicles and industries for controlling toxicity. In investigating the effect of optimal control, we have used one control at a time, the combination of two controls is used at a time while setting other(s) to zero to compare the effects of the control strategies on the eradication of threats to the system. Additionally, the case of all controls has also been taken into consideration. Our numerical results suggest that the use of two controls has highest impact on the control of the system threats. We have also shown through graphs that the prey population and predator population have decreased when the toxicity has increased. In FIGURE (3-9) we have observed that if controls are applied then the prey population and predator population significantly increases and in fig 10 we see that the effect of prey refuse is not remarkable. To find the optimum equilibrium level Pontryagin's maximum principle has been applied.

7. Acknowledgments

The first author gratefully acknowledges the financial support provided by the University Grant Commission, Bangladesh (UGC/1,157/ M.Phil and PhD/2016/5343, Date: 22/06/2016.)

Conflict of Interests

The authors declare that there is no conflict of interests.

References

[1] Chakravarty. K, Chakravarty, M. and Kar, T., Optimal Control of Harvest and Bifurcatin of a Prey-Predator Model with stage Structure, Appl. Math. Comput. 217 (2011), 8778–8792.

[2] T.D. Sagamiko, N. Shaban, C.L. Nahonyo, O.D. Makinde, Optimal Control of a Threatened Wildebeest-Lion Prey-Predator System in Serengeti Ecosystem, Open J. Ecol. 5 (2015), 110–119.

[3] M. Haque, E. , Ratio-dependent Predator-Prey Models of Interacting population, Bull. Math. Biol. 71(2) (2009), 430–452.

[4] Guin L.N, Mandal P.K, Effect of Prey refuge on Spatiotemporal dynamics of reaction-diffusion System, Comput. Math. Appl. 68(10) (2014), 1325–1340.

[5] Wang Y, Wang J, Influence of prey refuge on Predator-Prey Dynamics, Nonlinear Dyn. 67(1) (2012), 191–201.

[6] Alexander D. Bazykin, Nonlinear Dynamics of Interaction Population, Vol 11, World Scientific, (1998).

[7] G. Birkhoff, G.C. Rota, Ordinary Differential Equations, Ginn, Boston, (1982).

[8] J. Chattapadhyay, O. Arino, A predator–prey model with disease in the prey, Nonlinear Anal. 36 (1999), 747–766.

[9] J. Chattapadhyay, S. Pal, A. EI. Abdllaoui, Classical predator–prey system with infection of prey population– a mathematical model, Math. Methods Appl. Sci. 26 (2003), 1211–1222.

[10] Biswas M. H. A. and MdR de Pinho, A Maximum Principle for Optimal Control Problems with State and Mixed Constraints, ESAIM, Control Optim. Calc. Var. 21 (4) (2015), 939-957.

[11] Biswas M. H. A., A Necessary conditions for optimal control problems with and without state constraints: a comparative study, WSEAS Trans. Syst. Control, 6 (6) (2011), 217-228.

[12] Biswas M. H. A., Pinho MR de, A Non smooth Maximum Principle for Optimal Control Problems with State and Mixed Constraints–Convex Case, Discr. Contin. Dyn. Syst. (Special), (2011), 174-183.

[13] Biswas M. H. A., Pinho MR de, A variant of non smooth maximum principle for state constrained problems, IEEE 51st IEEE Conference on Decision and Control (CDC), (2012), 7685-7690.

[14] Biswas M. H. A., Haque M.M., Nonlinear Dynamical systems in Modeling and Control of Infectious Disease, Book chapter of differential and difference equations with applications, 164 (2016), 149-158.

[15] Pontryagin L. S., Boltyanskii V. G, Gamkrelize R. V, Mishchenko E. F., The Mathematical Theory of Optimal Processes, Wiley, New York, (1967).

[16] Lukes D. L, Differential Equations: Classical to Controlled, Academic Press, New York, (1982).

[17] Lenhart S, Workman J., Optimal Control Applied to Biological Models, Boca Raton, Chapmal Hall/CRC, (2007).

[18] Fleming W. H, Rishel R. W., Deterministic and Stochastic Optimal Control, Springer-Verlag, New York, (2005).

[19] Bolger, D., Newmark ,W., Morrison, T., and Doak , D. S.The need for integrative approaches to understand and conserve migratory ungulates, Ecol. Lett. (11) (2008), 63-77.